COMPUTER METHODS AND PROGRAMS IN BIOMEDICINE 130 (2016) 1–12

journal homepage: www.intl.elsevierhealth.com/journals/cmpb

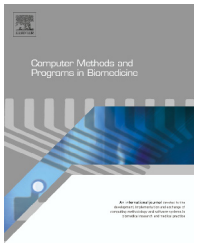

Quantification of knee vibroarthrographic signal irregularity associated with patellofemoral joint cartilage pathology based on entropy and envelope amplitude measures

Yunfeng Wu[a,b,*], *Pinnan Chen*[a], *Xin Luo*[a], *Hui Huang*[c], *Lifang Liao*[a], *Yuchen Yao*[a], *Meihong Wu*[a], *Rangaraj M. Rangayyan*[d]

[a] *School of Information Science and Technology, Xiamen University, 422 Si Ming South Road, Xiamen, Fujian 361005, China*
[b] *Fujian Key Laboratory of Sensing and Computing for Smart City, Xiamen University, 422 Si Ming South Road, Xiamen, Fujian 361005, China*
[c] *Department of Rehabilitation, Xiamen University Affiliated Zhongshan Hospital, 201 Hubin South Road, Xiamen, Fujian 361004, China*
[d] *Department of Electrical and Computer Engineering, Schulich School of Engineering, University of Calgary, Calgary, AB T2N 1N4, Canada*

ARTICLE INFO

Article history:
Received 18 August 2015
Received in revised form
12 March 2016
Accepted 16 March 2016

Keywords:
Approximate entropy
Articular cartilage
Fuzzy entropy
Knee joint
Symbolic entropy
Vibroarthrography

ABSTRACT

Background and objective: Injury of knee joint cartilage may result in pathological vibrations between the articular surfaces during extension and flexion motions. The aim of this paper is to analyze and quantify vibroarthrographic (VAG) signal irregularity associated with articular cartilage degeneration and injury in the patellofemoral joint.
Methods: The symbolic entropy (SyEn), approximate entropy (ApEn), fuzzy entropy (FuzzyEn), and the mean, standard deviation, and root-mean-squared (RMS) values of the envelope amplitude, were utilized to quantify the signal fluctuations associated with articular cartilage pathology of the patellofemoral joint. The quadratic discriminant analysis (QDA), generalized logistic regression analysis (GLRA), and support vector machine (SVM) methods were used to perform signal pattern classifications.
Results: The experimental results showed that the patients with cartilage pathology (CP) possess larger SyEn and ApEn, but smaller FuzzyEn, over the statistical significance level of the Wilcoxon rank-sum test ($p < 0.01$), than the healthy subjects (HS). The mean, standard deviation, and RMS values computed from the amplitude difference between the upper and lower signal envelopes are also consistently and significantly larger ($p < 0.01$) for the group of CP patients than for the HS group. The SVM based on the entropy and envelope amplitude features can provide superior classification performance as compared with QDA and GLRA, with an overall accuracy of 0.8356, sensitivity of 0.9444, specificity of 0.8, Matthews correlation coefficient of 0.6599, and an area of 0.9212 under the receiver operating characteristic curve.

* *Corresponding author at*: School of Information Science and Technology, Xiamen University, 422 Si Ming South Road, Xiamen, Fujian 361005, China. Tel.: +86 592 2194658.
E-mail address: y.wu@ieee.org (Y. Wu).
http://dx.doi.org/10.1016/j.cmpb.2016.03.021

Conclusions: The SyEn, ApEn, and FuzzyEn features can provide useful information about pathological VAG signal irregularity based on different entropy metrics. The statistical parameters of signal envelope amplitude can be used to characterize the temporal fluctuations related to the cartilage pathology.

1. Introduction

The knee joints bear almost the entire weight of the human body in daily activities, and they are vulnerable to different types of arthritis, such as osteoarthritis and rheumatoid arthritis [1]. Osteoarthritis could be the consequence of joint degeneration due to overloading activities with an aging phenomenon or physical injury in strenuous exercises [2]. Articular cartilage pathology is one of the most common degenerative disorders that may lead to the development of osteoarthritis in knees.

In most circumstances, a healthy knee with well-lubricated articular cartilage surfaces and intact menisci can perform smooth flexion and extension motions [3]. However, various pathological conditions of the knee joint, including chondromalacia, ruptured ligaments, and meniscal tears, may cause friction and grinding vibrations when the joint is articulated during daily activities such as walking, squatting, and swinging movement of the leg. The acceleration and vibratory signals of the knee joint, which are also referred to as vibroarthrographic (VAG) signals [4], can be recorded by inertial accelerometers in vibration arthrometry examinations [5]. Shark et al. [6] pointed out that the knee acoustic emission biomarkers are useful for quantitative assessment of joint degeneration, because the pathological VAG signals of knee-joint disorders commonly manifest different types of waveform complexity and frequency variations.

Recently, a number of published research works have advanced digital signal processing and pattern analysis technologies for VAG signal analysis. Rangayyan et al. [7] designed the autoregressive model to parameterize the stochastic process and the nonstationary nature of VAG signal segments. Krishnan et al. [8] and Kim et al. [9] computed optimized time-frequency distributions of VAG signals, and extracted the energy, energy spread, frequency, and frequency spread parameters to characterize the time-frequency variability of pathological signals. Rangayyan and Wu [10–12] proposed several temporal VAG signal features, such as form factor, variance of mean-squared (VMS) values, and signal turns count, along with a number of statistical features such as mean, standard deviation, coefficient of variation, skewness, kurtosis, Shannon information entropy, and Kullback–Leibler distance based on nonparametric Parzen-window probability density functions of VAG signals. Tanaka and Hoshiyama [13,14] compared the VAG signals of patients with high stages of osteoarthritis and those of age-matched healthy control subjects during standing-up and sitting-down movements, and reported that the powers of root-mean-squared (RMS) values are significantly greater in the frequency bands of 50–99 Hz and 100–149 Hz for symptomatic osteoarthritis knee joints. Rangayyan et al. [15] used the $1/f$ fractal model to compute the fractal dimension parameters of power spectral density from different segments of VAG signals. Baczkowicz et al. [16,17] studied age-dependent patellofemoral joint impairment by analyzing the VMS, entropy, difference between mean of four maximum and mean of four minimum values (R4), and the spectral power sums in two frequency bands of 50–250 Hz (P1) and 250–450 Hz (P2). Yang et al. [18] applied the detrended fluctuation analysis algorithm to derive the fractal scaling index parameter for quantification of intrinsic correlated signal fluctuations. The experimental results of Yang et al. [18] also showed that the pathological VAG signals of knee-joint disorders are commonly associated with significantly larger averaged envelope amplitude than the signals of healthy knees.

So far, plenty of previous works on screening of abnormal VAG signals associated with knee-joint disorders have been reported in the literature [19–25], there still calls for more computational methods for better quantification of knee-joint pathology. The aim of our present work only focuses on the analysis and quantification of VAG signal irregularity associated with articular cartilage degeneration and injury in the patellofemoral joint. We computed the symbolic entropy (SyEn), approximate entropy (ApEn), and fuzzy entropy (FuzzyEn) parameters to quantify the intrinsic irregularity in pathological VAG signals, and also measured three distinct envelope amplitude (EA) features to characterize the waveform variations and fluctuations in the time scale. Based on the entropy and envelope features, signal patterns can be effectively distinguished by using nonlinear classifiers.

2. Material and method

2.1. *Experiment*

We recruited 73 subjects to participate in the VAG signal acquisition experiments. The healthy subject (HS) group is composed of 55 control adults (28 males and 27 females) with normal knee-joint conditions, as confirmed by routine physical examinations and medical history records. The patient group consists of 18 subjects (9 males and 9 females) with cartilage pathology (CP) in their patellofemoral joints, the pathological conditions of which were assessed with magnetic resonance imaging examinations. The symptoms of the patients with cartilage disorders mainly contain chondromalacia patellae (CMP), softening of articular cartilage, and patellofemoral arthritis. Eleven CMP patients are with Grade I (3 cases, 2 males and 1 female), Grade II (3 cases, 3 females), Grade III (2 cases, 1 male and 1 female), and Grade IV (3 cases, 2 males and 1 female). There are 2 patients (1 male and 1 female)

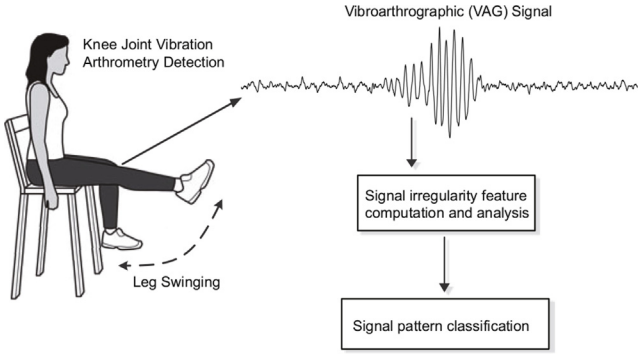

Fig. 1 – Pathological vibroarthrographic (VAG) signal of articular cartilage injury recorded in the knee-joint vibration arthrometry examination.

with articular cartilage softening, and 5 patients (3 males and 2 females) with patellofemoral arthritis. Patients suffering from other knee-joint disorders, such as meniscal tears and cruciate ligament injury, were excluded in the data acquisition experiments, because we just concentrated on the VAG signal irregularity as a result of the vibrations associated with articular cartilage disorders. All participants were able to voluntarily perform knee extension and flexion motions. The CP patients who cannot perform the knee extension motion from 90° to 0° or flexion motion from 0° to 90° as required by the experimental protocol were excluded in the present work. The age of the HS group (mean: 35.1 years; standard deviation, SD: 8.5 years) was comparable with that of the CP group (mean: 34.6 years; SD: 12.1 years). The subjects provided their informed and written consent documents as approved by the Ethics Committee of Xiamen University.

In the VAG signal acquisition experiments, the subjects sat on a rigid chair with both legs freely suspended in air, as illustrated in Fig. 1. Two triaxial accelerometer sensors (Model: xyzPlux, dimensions: 9 mm × 21 mm × 4 mm, weight: 1.9 g, PLUX Wireless Biosignals S.A., Lisbon, Portugal) were attached using two-sided adhesive tape on the proximal and middle positions of the patella, respectively. All subjects followed the experimental protocol to perform the knee motions of 90–0° extension and 0–90° flexion in the duration of 4 s (see Fig. 1). The raw VAG time series were recorded by the accelerometer (named as Sensor-I) at the middle-patella position, and the signals collected by the other accelerometer (named as Sensor-II) at the proximal-patella position were used to cancel the motion artifacts during knee motions. The signals were amplified by using a lightweight portable signal acquisition hub (Model: bioPLUX, dimensions: 82 mm × 54 mm × 15 mm, weight: 46 g, PLUX Wireless Biosignals S.A., Lisbon, Portugal). The signal data were acquired at the sampling rate of 1 kHz and wirelessly transferred to a computer with the Bluetooth v4.0 module, and digitized with a resolution of 12 bits per sample using the OpenSignals software platform (PLUX Wireless Biosignals S.A., Lisbon, Portugal). The digital values of each signal were converted into the amplitude unit of gravity force ($1\,g = 9.81\,m/s^2$).

In order to obtain high-quality VAG signals, we performed the necessary signal preprocessing procedures to remove the artifacts in the raw data. Motion artifacts in the VAG time series recorded from Sensor-I were canceled with the trend reference adaptively estimated from the signal recorded by Sensor-II. Baseline wander was eliminated in each VAG signal by using a cascade moving average filter [26]. Reduction of random noise was achieved with the combination of the ensemble empirical mode decomposition and detrended fluctuation analysis methods [27].

2.2. *Signal feature extraction*

We computed three entropy parameters, i.e., the SyEn, ApEn, and FuzzyEn, and three envelope parameters, i.e., the mean, SD, and RMS values of envelope amplitude, as the distinct features to characterize the irregular complexity of pathological VAG signals.

2.2.1. *Symbolic entropy*

The SyEn parameter represents the coarse graining of signal dynamics in a physiological process. Fig. 2 shows the signal symbolization procedures of quantization, word sequence segmentation, and entropy computation based on the probability density of words.

A temporal signal $\{x(n)\}$, $1 \le n \le N$, is required to be transformed into a number of symbol sequences $\{s^q(n)\}$, with a predefined amplitude threshold δ. The quantization parameter q determines the number of quantization levels for the conversion from the given signal to a symbol sequence. In the present work, the quantization parameter was set to be $q = 2$ such that the VAG signals can be symbolized as

$$s^q(n) = \begin{cases} 0, & |x(n) - \bar{x}| < \delta, \\ 1, & |x(n) - \bar{x}| \ge \delta, \end{cases} \tag{1}$$

where $\bar{x}$ is the mean of the VAG signal.

Typically, a word is defined to contain a sequential set of M signal symbols as $s_M^q(n) = \{s^q(n), s^q(n+1), \ldots, s^q(n+M-1)\}$. With the word length M, the total number of possible words that can appear in the symbol sequence is $W = q^M$. The probability of occurrence of each word is estimated throughout the entire symbol sequence $\{s_M^q(n)\}$ such that the probability density functions can be established. Then, the Shannon entropy can be calculated as

$$H_s(q, M) = -\sum_{b=1}^{W} P_b(s_M^q) \log_2 [P_b(s_M^q)], \tag{2}$$

where $P_b(s_M^q)$ is the probability of occurrence of a specified word.

Eguia et al. [28] reported that the empirical probability estimates of $P_b(s_M^q)$ may be biased due to systematic errors. Therefore, they proposed a correction to Shannon entropy by an additional bias term as [28]

$$H_c(q, M) = H_s(q, M) + \frac{W_R - 1}{2W \log_e 2}, \tag{3}$$

where W_R is the total number of words that actually appear in the symbol sequence $\{s_M^q(n)\}$. In this case, when the word

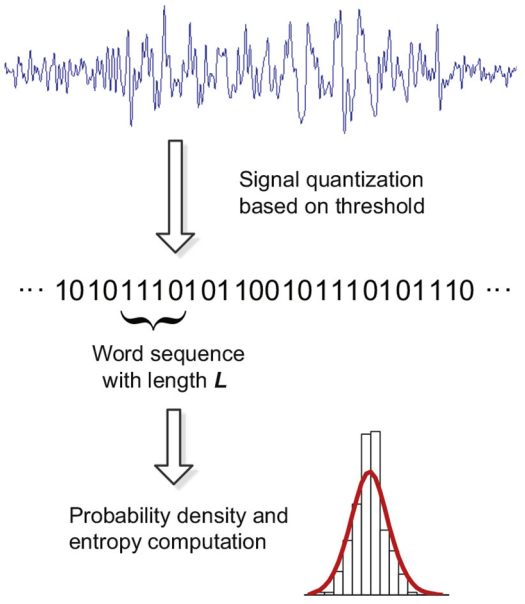

Fig. 2 – Diagram of the signal symbolization procedure that includes quantization, word sequence segmentation, probability density estimation, and entropy computation.

probability follows a uniform distribution, the maximum value of the corrected Shannon entropy can be derived as

$$H_c^{\max}(q, M) = \log_2 W + \frac{W-1}{2W\log_e 2}. \tag{4}$$

In order to ensure that the entropy values computed from two words with the same threshold and quantization parameters but different word length L are also comparable, Aziz and Arif [29] suggested that the corrected Shannon entropy should be normalized to produce the SyEn as

$$\begin{aligned} \mathrm{SyEn}(q, M) &= \frac{H_c(q, M)}{H_c^{\max}(q, M)} \\ &= \frac{H_s(q, M) + (W_R - 1)/(2W\log_e 2)}{\log_2 W + (W-1)/(2W\log_e 2)}. \end{aligned} \tag{5}$$

In the present study, we set the word length parameter to be $M=4$ such that the total number of possible words is $W=2^4=16$. The optimal threshold parameter was determined as $\delta=0.2\,g$, which was selected according to the smallest p value of the Wilcoxon rank-sum test (level of significant difference in statistics: $p<0.01$, implemented with IBM SPSS® Statistics, Version 20).

2.2.2. Approximate entropy

The ApEn parameter is a statistical measure proposed by Pincus [30], with the purpose of parameterizing the irregular dynamics in biomedical signals. Given an N-length signal, $\{x(n)\}$, the ApEn(i, t, N) model involves a positive integer $i \in \mathbb{Z}^+$ as the window length for similarity comparison, and a positive real value $t \in \Re^+$ as the tolerance threshold for similarity matching acceptance [31]. Let us define a vector sequence $\mathbf{u}^1(n)$, $\mathbf{u}^2(n)$, …, $\mathbf{u}^{(N-i+1)}(n)$, where each vector $\mathbf{u}^i(n) = [x(n), x(n+1), \ldots, x(n+i-1)]$ consists of i consecutive samples in the VAG signal. Then, we may calculate the maximum distance $d[\mathbf{u}^i(j), \mathbf{u}^i(k)]$, $1 \le j,\ k \le N-i+1$, between the elements from the vectors of $\mathbf{u}^i(j)$ and $\mathbf{u}^i(k)$ [32], as

$$d[\mathbf{u}^i(j), \mathbf{u}^i(k)] = \max_{l=1,2,\ldots,i} \left| x(j+l-1) - x(k+l-1) \right|. \tag{6}$$

Let $C_j^i(t)$ denote the probability of k satisfying the condition that the distance $d[\mathbf{u}^i(j), \mathbf{u}^i(k)]$ is smaller than t, as

$$C_j^i(t) = \frac{\text{number of } k \text{ satisfying } d[\mathbf{u}^i(j), \mathbf{u}^i(k)] < t}{N-i+1}, \tag{7}$$

which indicates the frequency of similarity between the vector $\mathbf{u}^i(k)$ and a given template $\mathbf{u}^i(j)$ within a tolerance threshold t. Define the function $\varphi^i(t)$ as the average of the natural logarithm values of $C_j^i(t)$ [33]:

$$\varphi^i(t) = \frac{\sum_{j=1}^{N-i+1} \log_e C_j^i(t)}{N-i+1}. \tag{8}$$

For a signal of a finite length, the corresponding approximate entropy, ApEn(i, t, N), can be computed as [31]

$$\begin{aligned} \mathrm{ApEn}(i, t, N) &= \varphi^i(t) - \varphi^{i+1}(t) \\ &= \frac{\sum_{j=1}^{N-i+1} \log_e C_j^i(t)}{N-i+1} - \frac{\sum_{j=1}^{N-i} \log_e C_j^{i+1}(r)}{N-i}. \end{aligned} \tag{9}$$

In general, a larger ApEn value indicates a relatively higher degree of irregularity or complexity in the signal.

In the present work, the ApEn model was used to parameterize the temporal regularity of VAG signals. The optimal combination of the ApEn parameters $i=4$ and $t=0.2\,g$ was obtained based on the results of the Wilcoxon rank-sum hypothesis test with the smallest p value (statistical significance level: $p<0.01$). The signal length $N=4000$ was identical for each VAG signal.

2.2.3. Fuzzy entropy

The FuzzyEn is a useful parameter that measures the self-similarity in a given signal $\{x(n)\}$ with a predefined fuzzy membership function [34,35]. Let us define a vector sequence, $\mathbf{y}^i(n) = [x(n),\ x(n+1), \ldots, x(n+i-1)] - \bar{x}^i(n)$, where $\bar{x}^i(n) = (1/i)\sum_{l=0}^{i-1} x(n+l)$ is the baseline within l signal samples such that each vector $\mathbf{y}^i(n)$ is free of local trend. The distance between $\mathbf{y}^i(j)$ and $\mathbf{y}^i(k)$ is measured with the maximum absolute difference $d_{j,k}^i = d[\mathbf{y}^i(j), \mathbf{y}^i(k)]$ express as

$$d_{j,k}^i = d[\mathbf{y}^i(j), \mathbf{y}^i(k)] = \max_{l=0,\ldots,i-1} |[x(j+l) - \bar{x}^i(j)] - [x(k+l) - \bar{x}^i(k)]| \tag{10}$$

Then, similarity degree is computed using an exponential formula $\mu(d_{j,k}^i, m, r)$ as the fuzzy membership function of the maximum distance, i.e.,

$$D_{j,k}^i(m, r) = \mu(d_{j,k}^i, m, r) = \exp\left[-\frac{(d_{j,k}^i)^m}{r} \right]. \tag{11}$$

We may define a function $\phi^i(m, r)$ to average all similarity measures $D^i_{j,k}(m, r)$ of a sequence of vectors $\mathbf{y}^i(j)$ as

$$\phi^i(m,r) = \frac{1}{N-i}\sum_{j=1}^{N-i}\left[\frac{1}{N-i-1}\sum_{k=1,k\neq j}^{N-i} D^i_{j,k}(m,r)\right], \tag{12}$$

$$\phi^{i+1}(m,r) = \frac{1}{N-i}\sum_{j=1}^{N-i}\left[\frac{1}{N-i-1}\sum_{k=1,k\neq j}^{N-i} D^{i+1}_{j,k}(m,r)\right] \tag{13}$$

For a signal $\{x(n)\}$ with the finite length N, the FuzzyEn is computed as

$$\text{FuzzyEn}(i, m, r, N) = \log_e\phi^i(m, \quad r) - \log_e\phi^{i+1}(m, \quad r) \tag{14}$$

We computed the FuzzyEn model with an exponential function as the fuzzy membership measure to represent the temporal complexity of VAG signals. The FuzzyEn embedding dimension was $i = 4$, and the exponential function parameters were set to be $m = 2$ and $r = 0.1 \times SD$, where SD is the standard deviation of the VAG signal to be analyzed.

2.2.4. *Envelope amplitude measurement*

Signal envelopes can be used to outline the temporal oscillations with large amplitude changes due to the vibrations occurring when areas of degenerated cartilage contact on the articular surfaces of a pathological knee joint [18]. In order to obtain the upper and lower envelopes in each VAG signal, we divided the signal into sequential non-overlapping segments, with an equal length of 20 samples for each. The local upper extreme (the highest peak) and the local lower extreme (the lowest trough) were then detected in each signal segment. Based on the local extremes detected, the samples between the sequential local extremes were estimated using the piecewise cubic Hermite interpolation method from one segment to another, for the upper and lower envelopes, respectively.

The EA feature is defined as the temporal difference between the upper and lower envelopes [18]. In the present study, the mean and SD values of EA were computed over the entire VAG signal for each subject. The RMS value of EA was also computed for each VAG signal as a measure of averaged signal power magnitude over a sample. As the statistical parameters that characterize the signal fluctuations associated with knee cartilage pathological conditions, the mean, SD, and RMS values of EA were used in the following pattern classification tasks, and denoted as EA-Mean, EA-SD, and EA-RMS, respectively.

2.3. *Pattern analysis and classifications*

2.3.1. *Quadratic discriminant analysis (QDA)*

Quadratic discriminant analysis (QDA) does not require the prior assumption that two subject groups have identical covariance matrices. The QDA method is the general form of Bayesian classification with a quadratic discriminant function that contains the second-order term as

$$J_c(\mathbf{y}) = -\frac{1}{2}\log_e\left|\sum_c\right| - \frac{1}{2}(\mathbf{y}-\mu_c)^T\sum_c^{-1}(\mathbf{y}-\mu_c) + \log_e\pi_c, \tag{15}$$

where $\sum_c$ represents the covariance matrix of each subject group ($c \in \{HS, CP\}$), μ_c is the group center (the mean vector of multivariate features), and π_c denotes the prior probability of each group (55/73 = 0.7534 and 18/73 = 0.2466 for the HS and CP subject groups, respectively). The signal pattern is categorized into the group c which maximizes the quadratic discriminant function, i.e., $\arg\max J_c(\mathbf{y})$. The QDA method allows flexibility for unequal covariance matrices of different classes, so it can fit imbalanced data better than linear discriminant analysis in practical applications. However, the QDA demands more computing resources to estimate the parameters in quadratic discrimination for each class.

2.3.2. *Generalized logistic regression analysis (GLRA)*

Generalized logistic regression analysis (GLRA) is a type of generalized linear modeling method that incorporates a multivariate linear model and a random variable to describe the systematic and random effects, respectively [36]. Because the VAG signal patterns belong to the groups of HS (with negative class label: −1) and CP (with positive class label: +1) subjects, a random variable with the Bernoulli distribution was chosen to compute the probabilities of the binomial groups. For the GLRA method, we used the logit link function, in the form of the natural logarithm of an odds ratio, to interpret the binomial relationship between the multivariate features and the estimated class probabilities p and $1-p$, i.e.,

$$\log_e\left(\frac{p}{1-p}\right) = \mathbf{y}^T\boldsymbol{\beta} = \beta_0 + y_1\beta_1 + \cdots + y_f\beta_f, \tag{16}$$

where the vector $\boldsymbol{\beta} = [\beta_0, \beta_1, \ldots, \beta_f]^T$ denotes the regression model coefficients, and $\mathbf{y} = [1, y_1, \ldots, y_f]^T$ is the GLRA input vector. In the present work, the input vector contains unity and the six features of SyEn, ApEn, FuzzyEn, EA-Mean, EA-SD, and EA-RMS. We applied the iterative weighted least-squares procedure [37] to compute the maximum likelihood estimates of the GLRA coefficients. The optimal GLRA regression coefficients were $\boldsymbol{\beta}^* = [22.55, 30.73, 648.06, -108.41, -331.32, -464.82, 482.1]^T$, which is expected to help the GLRA achieve the largest area under the receiver operating characteristic (ROC) curve.

2.3.3. *Support vector machine (SVM)*

We employed the support vector machine (SVM) to perform nonlinear classification of VAG signal patterns. The SVM is an artificial neural network paradigm that is established with the Vapnik–Chervonenkis dimension theory to avoid the curse of dimensionality problem [38]. The SVM searches for a number of training data patterns as informative support vectors to construct a maximal margin hyperplane between different classes. For nonlinearly separable data, the SVM projects its inputs onto a high-dimensional space using nonlinear kernel functions, and then adjusts the mapped patterns to be linearly separable with several slack variables.

The optimization of the SVM network is equivalent to a quadratic programming problem in relation to the objective function of maximum margin and the modified equality constraints with slack variables. Then, the optimal solutions of SVM parameters can be obtained by solving the dual quadratic programming problem with Lagrange multipliers under the Karush–Kuhn–Tucker condition [39].

The features sent to the SVM inputs were the SyEn, ApEn, FuzzyEn, EA-Mean, EA-SD, and EA-RMS, the same as for the GLRA method. The nonlinear mapping of input features to the high-dimensional space was performed with the Gaussian kernel function as $\kappa(\mathbf{y}, \mathbf{y}_f) = \exp(-\|\mathbf{y} - \mathbf{y}_f\|^2/\sigma^2)$. We searched the spread parameter σ from 1 to 100 in our experiments, and selected the optimal value of $\sigma = 5$ that could assist the SVM to achieve the largest value of area under the ROC curve.

2.3.4. *Classification performance evaluation*

In order to test the generalization ability of the aforementioned classification methods, we applied the leave-one-out cross-validation approach for classification performance evaluation. In each cross-validation step, one signal pattern is excluded from the classifier training process and then distinguished separately. Such steps proceed until all signal patterns have been categorized one by one.

The ROC curves were generated for the pattern classifiers, and the areas under the curve (AUC) were estimated to represent the diagnostic performance. The optimal cutoff point in the ROC curve for the binary classification decision of each classifier was determined according to the maximum value of Youden's index [40], J, i.e.,

$$\max J = \text{Sensitivity} + \text{Specificity} - 1. \tag{17}$$

The confusion matrix was calculated for each classification method, with the ratios of true positive (TP), true negative (TN), false positive (FP), and false negative (FN). The classification results in terms of sensitivity, specificity, and overall accuracy were derived from the confusion matrix.

In addition, Matthews correlation coefficient (MCC) [41] was calculated as a classification quality indicator for performance evaluation:

$$\text{MCC} = \frac{\text{TP} \times \text{TN} - \text{FP} \times \text{FN}}{\sqrt{P(1-P)S(1-S)}}, \tag{18}$$

$$P = (\text{TP} + \text{FP})/(\text{TP} + \text{FP} + \text{TN} + \text{FN}), \tag{19}$$

$$S = (\text{TP} + \text{FN})/(\text{TP} + \text{FP} + \text{TN} + \text{FN}). \tag{20}$$

The MCC parameter has the major advantage of involving all the true and false positives and negatives in the correlation coefficient form to provide the evaluation of binary classification outcomes [41]. Typically, a zero MCC value implies that a binary classification is equivalent to random guess. A positive value of MCC indicates proper classification, and perfect classification is achieved when MCC is equal to +1. On the other hand, a negative MCC value represents a poor classification worse than random guess (MCC = −1 denotes a total disagreement between the predicted and actual groups).

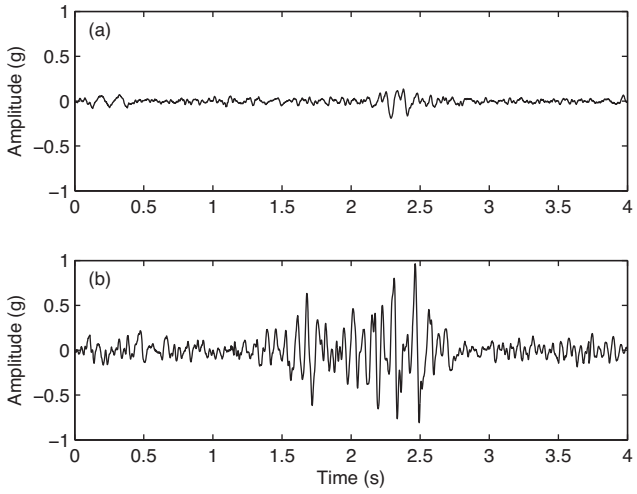

Fig. 3 – Knee-joint vibroarthrographic (VAG) signals of (a) a 34-year-old healthy male subject and (b) a 33-year-old male patient with chondromalacia patellae grade III, after signal preprocessing for baseline wander removal and random noise reduction.

3. Results

Fig. 3 displays the artifact-free VAG signals of a healthy subject and a patient with symptoms of CMP (grade III). It can be observed from Fig. 3 that the temporal waveform portion from 1.35 to 2.73 s related to the pathological condition exhibits large and irregular oscillations. Fig. 4 illustrates the upper and lower envelopes estimated from the VAG signals of the healthy subject and CMP patient as shown in Fig. 3. It can be observed in Fig. 4 that the boundaries of signal oscillations in the time scale have been effectively sketched by the upper and lower envelopes.

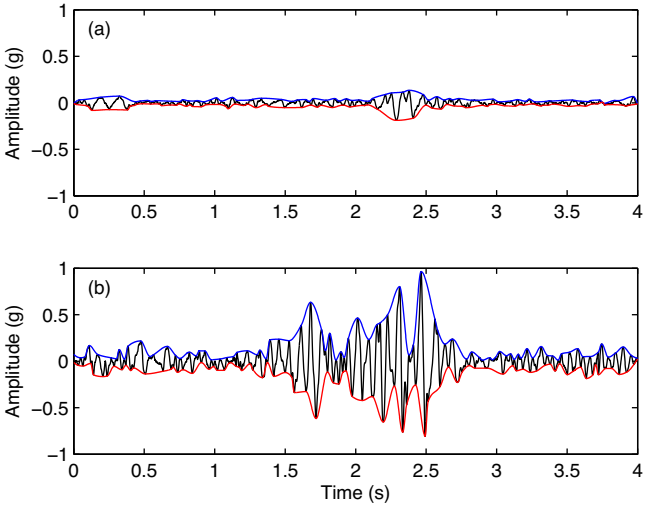

Fig. 4 – Upper and lower envelopes detected from the vibroarthrographic (VAG) signals of (a) a 34-year-old healthy male subject and (b) a 33-year-old male patient with chondromalacia patellae at grade III stage.

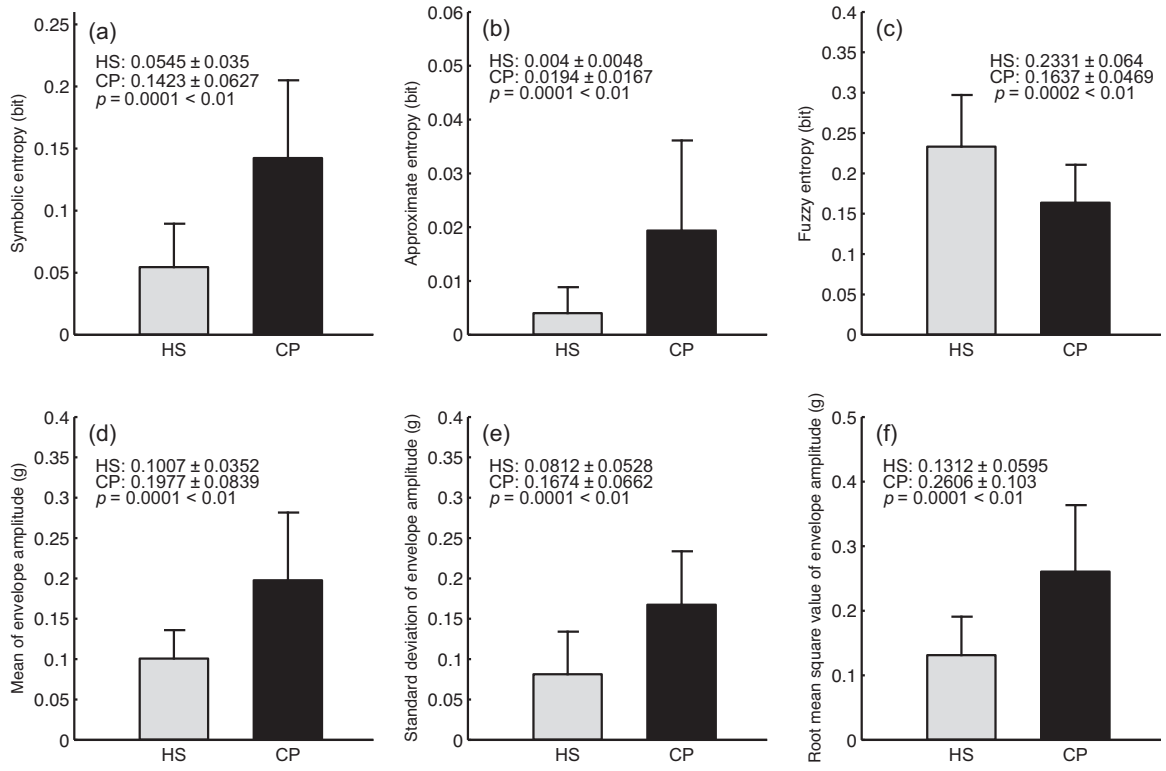

Fig. 5 – Statistics of entropy and envelope amplitude parameters for the groups of healthy subjects (HS) and patients with patellofemoral joint cartilage pathology (CP): (a) symbolic entropy (SyEn), (b) approximate entropy (ApEn), (c) fuzzy entropy (FuzzyEn), (d) mean of envelope amplitude (EA-Mean), (e) standard deviation of envelope amplitude (EA-SD), and (f) root-mean-squared value of envelope amplitude (EA-RMS). Statistical significance level of the Wilcoxon rank-sum hypothesis test: $p < 0.01$.

In Figs. 3 and 4, it can be observed that the pathological VAG signal contains more fluctuations related to the corresponding CP conditions. Fig. 5 shows the bar graphics of the statistics of the entropy parameters and envelope amplitude measures. It is clear that the parameters of SyEn, ApEn, EA-Mean, EA-SD, and EA-RMS are consistently larger for CP patients, over the statistical significance level of $p < 0.01$ in the Wilcoxon rank-sum test. The averaged SyEn of the CP group (SyEn mean: 0.1423 bit) is 2.6 times the corresponding value of the HS group (SyEn mean: 0.0545 bit). Such a result implies that the VAG signals of CP patients commonly contain more components of chaotic dynamics than the signals of healthy adults. The ApEn mean value of CP patients is also 4.85 times higher than that of the HS participants, which indicates that the knee-joint pathological conditions associated with CP may cause substantial irregular oscillations over the predefined threshold of 0.2 g in the VAG signals. The SD of a pathological VAG signal is commonly larger than that of a healthy signal, such that the fuzzy exponential function for the pathological signal is also extended with a wider boundary, which is determined by the parameter $r = 0.1 \times SD$. Because the FuzzyEn of the pathological VAG signal would be decreased due to the extended fuzzy similarity tolerance, the FuzzyEn mean value of CP patients becomes significantly smaller ($p = 0.0002$) than that of the HS participants.

The envelope amplitude parameters, in terms of EA-Mean, EA-SD, and EA-RMS, provide similar results as well. The EA-Mean parameter describes the averaged difference of signal amplitude between the upper and lower envelopes, as depicted in Fig. 4. It is noted that the EA-Mean values of the VAG signals in CP patients (mean ± SD: 0.1977 ± 0.0839 g) are much larger than those values in HS (mean ± SD: 0.1007 ± 0.0352 g) in the statistical sense. The EA-SD parameter represents the irregularity of temporal fluctuations caused by the pathological conditions of CP. The averaged EA-SD value of the CP patient group is 0.1674 g, twice larger than that of the HS group (EA-SD mean: 0.0812 g), which shows that the variations of envelope amplitude fluctuations are also high in the VAG signals of CP patients. In addition, the VAG signals of CP patients possess significantly larger EA-RMS value (mean ± SD: 0.2606 ± 0.103 g) in comparison with that of HS participants (mean ± SD: 0.1312 ± 0.0595 g). It can be inferred that each data sample of pathological VAG signals may contain more averaged signal power in magnitude.

Fig. 6 and Table 1 provide the gender-dependent statistical results of the entropy and envelope amplitude parameters computed for the male and female subjects in the HS and CP groups, respectively. It is worth noting in Fig. 6 that there is no visible difference of any of six VAG signal irregular parameters between the male and female control subjects in the HS group, but the mean values of SyEn, ApEn, EA-Mean, EA-SD, and EA-RMS of male patients are a bit larger than those of female patients in the CP group. The FuzzyEn results are comparable between male and female subjects in both of the HS and CP

Table 1 – Statistical values of entropy and envelope amplitude parameters for the male and female subjects in the groups of healthy subjects (HS) and patients with patellofemoral joint cartilage pathology (CP).

Subject group	Features	Statistics (mean ± standard deviation)		p value
		Male	Female	
HS	SyEn (bit)	0.0567 ± 0.0354	0.0521 ± 0.0351	0.6279
	ApEn (bit)	0.004 ± 0.0042	0.0041 ± 0.0054	0.9323
	FuzzyEn (bit)	0.2382 ± 0.0579	0.2278 ± 0.0706	0.5497
	EA-Mean (g)	0.1042 ± 0.0376	0.0971 ± 0.0328	0.4577
	EA-SD (g)	0.0779 ± 0.0379	0.0846 ± 0.0653	0.6419
	EA-RMS (g)	0.1309 ± 0.0513	0.1315 ± 0.068	0.9726
CP	SyEn (bit)	0.1584 ± 0.0757	0.1262 ± 0.045	0.2879
	ApEn (bit)	0.023 ± 0.0212	0.0157 ± 0.0107	0.3709
	FuzzyEn (bit)	0.1608 ± 0.0496	0.1666 ± 0.0467	0.8016
	EA-Mean (g)	0.2229 ± 0.1027	0.1725 ± 0.0546	0.212
	EA-SD (g)	0.1823 ± 0.0842	0.1526 ± 0.0415	0.3575
	EA-RMS (g)	0.2889 ± 0.1304	0.2322 ± 0.061	0.9726

SyEn, symbolic entropy; ApEn, approximate entropy; FuzzyEn, fuzzy entropy; EA, envelope amplitude; SD, standard deviation; RMS, root mean square value.
Statistical significant difference of the two-sample t-test hypothesis test: $p < 0.05$.

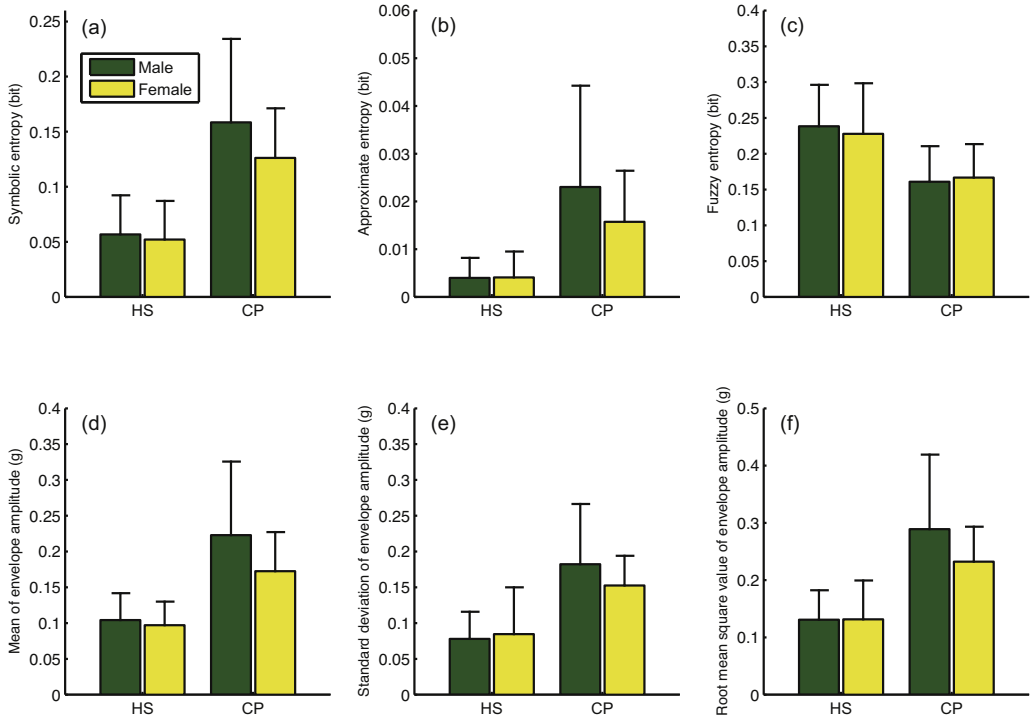

Fig. 6 – Gender-dependent statistics of entropy and envelope amplitude parameters for the groups of healthy subjects (HS) and patients with patellofemoral joint cartilage pathology (CP): (a) symbolic entropy (SyEn), (b) approximate entropy (ApEn), (c) fuzzy entropy (FuzzyEn), (d) mean of envelope amplitude (EA-Mean), (e) standard deviation of envelope amplitude (EA-SD), and (f) root-mean-squared value of envelope amplitude (EA-RMS). Details of statistical values are provided in Table 1.

groups. In order to compare the mean difference of the gender-dependent parameters in statistical sense, we computed the two-sample t-test of each parameter between the male and female subjects in both of HS and CP groups, respectively. The null hypothesis of the two-sample t-test is that the parameters of male and female subjects are from normal distributions with equal means, against the alternative hypothesis that the parameter means of male and female subjects are not equal, with a statistical significance level of $p < 0.05$. According to Table 1, we may observe that none of six parameters indicate a statistically significant difference between the male and female patients. The experimental results suggest that the VAG signals of male patients with patellofemoral joint CP conditions commonly tend to be with a slightly higher degree

Table 2 – Vibroarthrographic (VAG) signal classification results obtained with the quadratic discriminant analysis (QDA), generalized logistic regression analysis (GLRA), and support vector machine (SVM) methods for the groups of healthy subjects (HS) and patients with patellofemoral joint cartilage pathology (CP).

Classification results	QDA	GLRA	SVM
Sensitivity	0.7222	0.7222	0.9444
Specificity	0.8545	0.9091	0.8
Accuracy	0.8219	0.863	0.8356
AUC	0.8793	0.9111	0.9212
MCC	0.5492	0.6313	0.6599

AUC, area under the receiver operating characteristic curve; MCC, Matthews correlation coefficient.

of irregularity than the signals of female patients, but such a difference is still not evident enough between male and female patients. It is therefore no necessary to isolate the male and female subjects in follow-up VAG signal pattern classification.

In addition, we compared the male-to-male and female-to-female signal feature differences between the CP and HS groups, respectively. It is noted that male-to-male differences of SyEn (CP versus HS: 0.1017 bit), ApEn (CP versus HS: 0.019 bit), FuzzyEn (HS versus CP: 0.0774 bit), EA-Mean (CP versus HS: 0.1187 *g*), EA-SD (CP versus HS: 0.1044 *g*), and EA-RMS (CP versus HS: 0.158 *g*), are consistently larger than the female-to-female differences of SyEn (CP versus HS: 0.0741 bit), ApEn (CP versus HS: 0.0116 bit), FuzzyEn (HS versus CP: 0.0612 bit), EA-Mean (CP versus HS: 0.0754 *g*), EA-SD (CP versus HS: 0.068 *g*) and EA-RMS (CP versus HS: 0.1007 *g*). Such results suggest that the differences of six features become much larger for the male subjects than the females, when their knee joints are affected by the pathological changes of articular cartilage.

Based on the distinct features that characterize temporal complexity of abnormal signals, the QDA, GLRA, and SVM methods are able to provide CP signal pattern classification with good performance. Table 2 lists the classification results computed from the confusion matrices of the three classifiers. The GLRA classifier provided an overall accuracy of 0.863 for the set of 73 VAG signals, slightly better than the results of the SVM (accuracy: 0.8356) and the QDA (accuracy: 0.8219) approaches. The SVM provided the sensitivity of 0.9444, which was better than the QDA (sensitivity: 0.7222) and the GLRA (sensitivity: 0.7222). The classification results shown in Fig. 7 indicate that the SVM with Gaussian kernels has a better ability to distinguish the pathological VAG signals of CP patients. On the other hand, the GLRA can provide a specificity value of 0.9091, superior to the QDA (specificity: 0.8545) and the SVM (specificity: 0.8), which implies that the GLRA is more sensitive to the normal signal patterns of HS participants. As shown in Fig. 8, the SVM outperforms the QDA and GLRA methods with a prominent receiver operating characteristic (ROC) curve and superior area under the curve (AUC) of 0.9212 (standard error, SE: 0.0306). The GLRA produces a comparable ROC curve with the AUC of 0.9111 (SE: 0.0379), whereas the QDA has the lowest AUC value of 0.8793 (SE: 0.0423). Moreover, the SVM provides the highest MCC result of 0.6599 over the other two classifiers

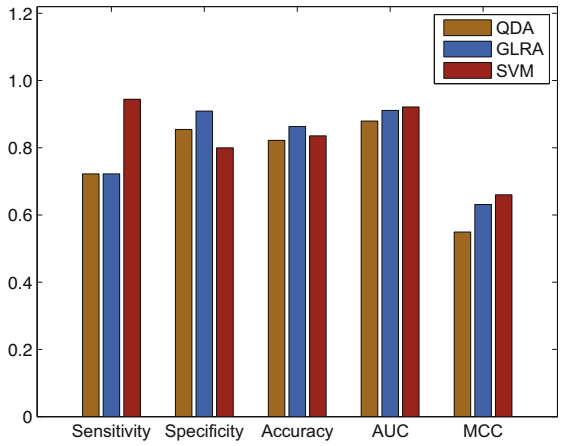

Fig. 7 – Bar graph results, in terms of sensitivity, specificity, overall accuracy, area under the receiver operating characteristic curve (AUC), and Matthews correlation coefficient (MCC), provided by the quadratic discriminant analysis (QDA), generalized logistic regression analysis (GLRA), and support vector machine (SVM) methods, for vibroarthrographic (VAG) signal classification.

(QDA MCC: 0.5492, GLRA MCC: 0.6313), which also confirms the merits of the SVM method for pathological VAG signal pattern classification. For the purpose of comparison, we computed the ROC results of the popular naive Bayes and *k*-nearest neighbor (*k*-NN, $k=5$) classifiers, which were also evaluated by the leave-one-out cross-validation method. The AUC values of naive Bayes and *k*-NN classifiers were 0.7953 and 0.8325, respectively, either of which is lower than that of the QDA, GLRA or SVM classifier.

In comparison with the ROC results reported in the previous studies with 89 VAG signals, the AUC value of the SVM classifier, input with the six features developed in the

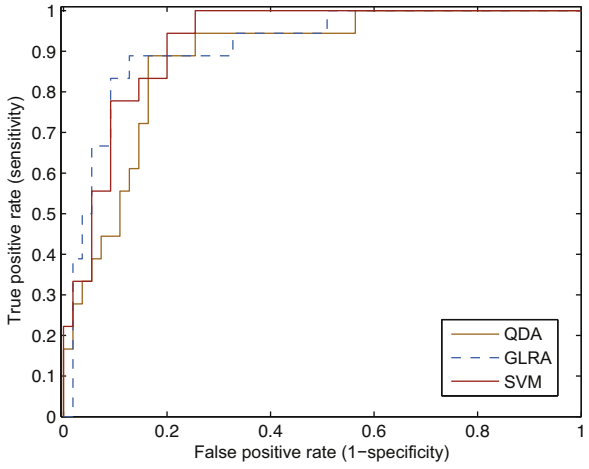

Fig. 8 – Receiver operating characteristic (ROC) curves generated by the quadratic discriminant analysis (QDA; area under ROC curve: 0.8793), generalized logistic regression analysis (GLRA; area under ROC curve: 0.9111), and support vector machine (SVM; area under ROC curve: 0.9212) methods.

present study, is higher than that of the radial basis function network input with the features of form factor, skewness, kurtosis, Shannon entropy (AUC: 0.82) [10], with the features of turns count and variance of mean-squared values (AUC: 0.9174) [11], or with difference between the Kullback–Leibler distances of the normal and abnormal signal probability density functions (PDFs), mean, and standard deviation of signal PDFs (AUC: 0.8322) [12]. The dynamic weighted classifier fusion system proposed by Cai et al. [23], input with the features of the atom number of wavelet matching pursuit decomposition and turns count with the fixed threshold, can demonstrate the merits of multiple classifier systems with a better ROC result (AUC: 0.9515), which shows the direction of signal classification performance improvement in the future work.

4. Discussion and conclusion

The measures of SyEn, ApEn, and FuzzyEn can parameterize the signal fluctuations of pathological VAG signals with measures of entropy, and the EA-Mean, EA-SD, and EA-RMS parameters characterize the nature of oscillations associated with the CP conditions in the time scale.

The SyEn measure is an informative parameter in signal dynamics analysis. The SyEn symbolization procedure converts the signal samples into a set of word sequences, and then computes the Shannon entropy with respect to the probabilities of word sequences. Regarding the signal quantization threshold, Aziz and Arif [29] pointed out that a small threshold value would measure the noise-related oscillations as a part of signal fluctuations, whereas a large quantization threshold might not represent the details of subtle variations caused by the pathological conditions of CP in the present work. In our experiments, the optimal quantization threshold of 0.2 g, which was determined with the Wilcoxon rank-sum test results, can help the SyEn parameter achieve excellent interclass separation between the groups of HS participants and CP patients in statistical sense. SyEn also provides useful information for temporal signal analysis with appropriate word sequences. The length of word sequence in our study is $M = 4$, which corresponds a time span of 4 ms in the signal (with the sampling rate of 1 kHz). In future work, we could study the instantaneous signal power changes along different segments, each with the time span of 4 ms, in a VAG signal.

The ApEn parameter has the merit of relatively lower computational requirement, with favorable robustness to random noise as well. A limitation of ApEn is that the entropy computing procedure avoids the occurrence of $\log_e(0)$, which might lead to some bias for signals of different length. In the present study, all VAG signals are with the same length, so the ApEn bias effect is small and the results are comparable between the HS and CP groups.

The EA-Mean parameter characterizes the averaged amplitude difference between the upper and lower envelopes over the entire VAG signal. The EA-Mean results indicate that the vibrations related to CP conditions in the knee may result in some oscillations with large amplitude differences. On the other hand, the EA-SD parameter results imply the irregularity of oscillation occurrences during knee flexion and extension motions. The EA-RMS results show that the abnormal VAG signals of CP patients commonly contain larger averaged signal power per sample than the HS signals. All of these three envelope amplitude parameters are well-suited for representation of subtle fluctuations of pathological VAG signals in the time domain.

The present work has some limitations with a relatively small data set of subjects. In our experiments, we only focused on the quantification of abnormal VAG signal irregularity due to CP vibrations in the patellofemoral joint, rather than the various types of signal complexity related to other pathological conditions. Therefore, we had to include a limited number of CP patients who do not suffer from other knee-joint disorders such as tear of the meniscus, bony spurs, medial synovial plica, or cruciate ligament injuries. The pilot data recorded in the present experiment were not sufficient enough to create precise the correlations with the grade of cartilage pathology in the patellofemoral joint in statistical sense.

Vibration arthrometry is a complementary technique for diagnosis of articular cartilage pathology [42]. In the present work, we computed the SyEn, ApEn, FuzzyEn, EA-Mean, EA-SD, and EA-RMS parameters as distinct signal features. The SVM method achieved pattern classification results with excellent sensitivity, AUC, and MCC values. Our efforts assist to quantify the pathological signal irregularity of CP-related vibrations during knee flexion and extension motions, with high diagnostic performance. Of course, an accurate assessment of knee-joint CP conditions in clinical practice still calls for more advanced machine learning methods. In the next step of signal pattern analysis, we are also interested to consider more advanced machine learning approaches to effectively distinguish multiple knee-joint symptoms.

Competing interests

There is no conflict of interest.

Ethical approval

The experiment protocol and subject consent documents were approved by the Ethics Committee of Xiamen University.

Acknowledgments

The authors would like to express their gratitude to anonymous reviewers for their constructive comments and Ms. Hang Zhang for technical assistance. This work has been supported by the National Natural Science Foundation of China (grant numbers: 81101115, 81272168, and 31200769). Yunfeng Wu and Meihong Wu were supported by the Program for New Century Excellent Talents in Fujian Province University. Rangaraj M. Rangayyan was supported by the High-Level Foreign Experts Program of the State Administration of Foreign Experts Affairs in China.

REFERENCES

[1] M. Bonnin, P. Chambat, Osteoarthritis of the Knee, Springer, New York, NY, 2008.
[2] Y. Wu, Knee Joint Vibroarthrographic Signal Processing and Analysis, Springer-Verlag, Heidelberg, Germany, 2015.
[3] Y. Wu, S. Krishnan, R.M. Rangayyan, Computer-aided diagnosis of knee-joint disorders via vibroarthrographic signal analysis: a review, Crit. Rev. Biomed. Eng. 38 (2) (2010) 201–224.
[4] R.M. Rangayyan, Biomedical Signal Analysis, 2nd ed., IEEE Press and Wiley, New York, NY, 2015.
[5] S.C. Abbott, M.D. Cole, Vibration arthrometry: a critical review, Crit. Rev. Biomed. Eng. 41 (3) (2013) 223–242.
[6] L.-K. Shark, H. Chen, J. Goodacre, Knee acoustic emission: a potential biomarker for quantitative assessment of joint ageing and degeneration, Med. Eng. Phys. 33 (5) (2011) 534–545.
[7] R.M. Rangayyan, S. Krishnan, G.D. Bell, C.B. Frank, K.O. Ladly, Parametric representation and screening of knee joint vibroarthrographic signals, IEEE Trans. Biomed. Eng. 44 (11) (1997) 1068–1074.
[8] S. Krishnan, R.M. Rangayyan, G.D. Bell, C.B. Frank, Adaptive time-frequency analysis of knee joint vibroarthrographic signals for noninvasive screening of articular cartilage pathology, IEEE Trans. Biomed. Eng. 47 (6) (2000) 773–783.
[9] K.S. Kim, J.H. Seo, J.U. Kang, C.G. Song, An enhanced algorithm for knee joint sound classification using feature extraction based on time-frequency analysis, Comput. Methods Progr. Biomed. 94 (2) (2009) 198–206.
[10] R.M. Rangayyan, Y.F. Wu, Screening of knee-joint vibroarthrographic signals using statistical parameters and radial basis functions, Med. Biol. Eng. Comput. 46 (3) (2008) 223–232.
[11] R.M. Rangayyan, Y. Wu, Analysis of vibroarthrographic signals with features related to signal variability and radial-basis functions, Ann. Biomed. Eng. 37 (1) (2009) 156–163.
[12] R.M. Rangayyan, Y. Wu, Screening of knee-joint vibroarthrographic signals using probability density functions estimated with Parzen windows, Biomed. Signal Process. Control 5 (1) (2010) 53–58.
[13] N. Tanaka, M. Hoshiyama, Articular sound and clinical stages in knee arthropathy, J. Musculoskelet. Res. 14 (1) (2011) 1150006.
[14] N. Tanaka, M. Hoshiyama, Vibroarthrography in patients with knee arthropathy, J. Back Musculoskelet. Rehabil. 25 (2) (2012) 117–122.
[15] R.M. Rangayyan, F. Oloumi, Y. Wu, S. Cai, Fractal analysis of knee-joint vibroarthrographic signals via power spectral analysis, Biomed. Signal Process. Control 8 (1) (2013) 26–29.
[16] D. Baczkowicz, E. Majorczyk, Joint motion quality in vibroacoustic signal analysis for patients with patellofemoral joint disorders, BMC Musculoskelet. Disord. 15 (2014) 426.
[17] D. Baczkowicz, E. Majorczyk, K. Krecisz, Age-related impairment of quality of joint motion in vibroarthrographic signal analysis, BioMed Res. Int. 2015 (2015) 591707.
[18] S. Yang, S. Cai, F. Zheng, Y. Wu, K. Liu, M. Wu, Q. Zou, J. Chen, Representation of fluctuation features in pathological knee joint vibroarthrographic signals using kernel density modeling method, Med. Eng. Phys. 36 (10) (2014) 1305–1311.
[19] Z.M.K. Moussavi, R.M. Rangayyan, G.D. Bell, C.B. Frank, K.O. Ladly, Y.T. Zhang, Screening of vibroarthrographic signals via adaptive segmentation and linear prediction modeling, IEEE Trans. Biomed. Eng. 43 (1) (1996) 15–23.
[20] K. Umapathy, S. Krishnan, Modified local discriminant bases algorithm and its application in analysis of human knee joint vibration signals, IEEE Trans. Biomed. Eng. 53 (3) (2006) 517–523.
[21] T. Mu, A.K. Nandi, R.M. Rangayyan, Screening of knee-joint vibroarthrographic signals using the strict 2-surface proximal classifier and genetic algorithm, Comput. Biol. Med. 38 (10) (2008) 1103–1111.
[22] Y. Wu, S. Krishnan, Combining least-squares support vector machines for classification of biomedical signals: a case study with knee-joint vibroarthrographic signals, J. Exp. Theor. Artif. Intell. 23 (1) (2011) 63–77.
[23] S. Cai, S. Yang, F. Zheng, M. Lu, Y. Wu, S. Krishnan, Knee joint vibration signal analysis with matching pursuit decomposition and dynamic weighted classifier fusion, Comput. Math. Methods Med. 2013 (2013) 904267.
[24] Y. Wu, S. Cai, S. Yang, F. Zheng, N. Xiang, Classification of knee joint vibration signals using bivariate feature distribution estimation and maximal posterior probability decision criterion, Entropy 15 (4) (2013) 1375–1387.
[25] W.-C. Lin, T.-F. Lee, S.-Y. Lin, L.-F. Wu, H.-Y. Wang, L. Chang, J.-M. Wu, J.-C. Jiang, C.-C. Tuan, M.-F. Horng, C.-S. Shieh, P.-J. Chao, Non-invasive knee osteoarthritis diagnosis via vibroarthrographic signal analysis, J. Inform. Hiding Multimed. Signal Process. 5 (3) (2014) 497–507.
[26] S. Cai, Y. Wu, N. Xiang, Z. Zhong, J. He, L. Shi, F. Xu, Detrending knee joint vibration signals with a cascade moving average filter, in: Proceedings of the 34th Annual International Conference of IEEE Engineering in Medicine and Biology Society, San Diego, CA, USA, 2012, pp. 4357–4360.
[27] Y. Wu, S. Yang, F. Zheng, S. Cai, M. Lu, M. Wu, Removal of artifacts in knee joint vibroarthrographic signals using ensemble empirical mode decomposition and detrended fluctuation analysis, Physiol. Measur. 35 (3) (2014) 429–439.
[28] M.C. Eguia, M.I. Rabinovich, H.D.I. Abarbanel, Information transmission and recovery in neural communication channels, Phys. Rev. E 62 (5) (2000) 7111–7122.
[29] W. Aziz, M. Arif, Complexity analysis of stride interval time series by threshold dependent symbolic entropy, Eur. J. Appl. Physiol. 98 (1) (2006) 30–40.
[30] S.M. Pincus, Approximate entropy as a measure of system complexity, Proc. Natl. Acad. Sci. U. S. A. 88 (6) (1991) 2297–2301.
[31] S.M. Pincus, A.L. Goldberger, Physiological time-series analysis: what does regularity quantify? Am. J. Physiol. 266 (4) (1994) 1643–1656.
[32] S.M. Pincus, Approximate entropy (ApEn) as a complexity measure, Chaos 5 (1) (1995) 110–117.
[33] J.S. Richman, J.R. Moorman, Physiological time-series analysis using approximate entropy and sample entropy, Am. J. Physiol. 278 (6) (2000) 2039–2049.
[34] W. Chen, Z. Wang, H. Xie, W. Yu, Characterization of surface EMG signal based on fuzzy entropy, IEEE Trans. Neural Syst. Rehabil. Eng. 15 (2) (2007) 266–272.
[35] W. Chen, J. Zhuang, W. Yu, Z. Wang, Measuring complexity using FuzzyEn, ApEn, and SampEn, Med. Eng. Phys. 31 (1) (2009) 61–68.
[36] H. Madsen, P. Thyregod, Introduction to General and Generalized Linear Models, CRC Press, Boca Raton, FL, 2011.
[37] A. Charnes, E.L. Frome, P.L. Yu, The equivalence of generalized least squares and maximum likelihood estimates in the exponential family, J. Am. Stat. Assoc. 71 (353) (1976) 169–171.
[38] W.S. Noble, What is a support vector machine? Nature Biotechnol. 24 (12) (2006) 1565–1567.
[39] C.J.C. Bugers, A tutorial on support vector machines for pattern recognition, Data Min. Knowl. Discov. 2 (2) (1998) 121–167.

[40] W.J. Youden, Index for rating diagnostic tests, Cancer 3 (1) (1950) 32–35.
[41] P. Baldi, S. Brunak, Y. Chauvin, C.A.F. Andersen, H. Nielsen, Assessing the accuracy of prediction algorithms for classification: an overview, Bioinformatics 16 (5) (2000) 412–424.
[42] N.P. Reddy, B.M. Rothschild, E. Verrall, A. Joshi, Noninvasive measurement of acceleration at the knee joint in patients with rheumatoid arthritis and spondyloarthropathy of the knee, Ann. Biomed. Eng. 29 (12) (2001) 1106–1111.